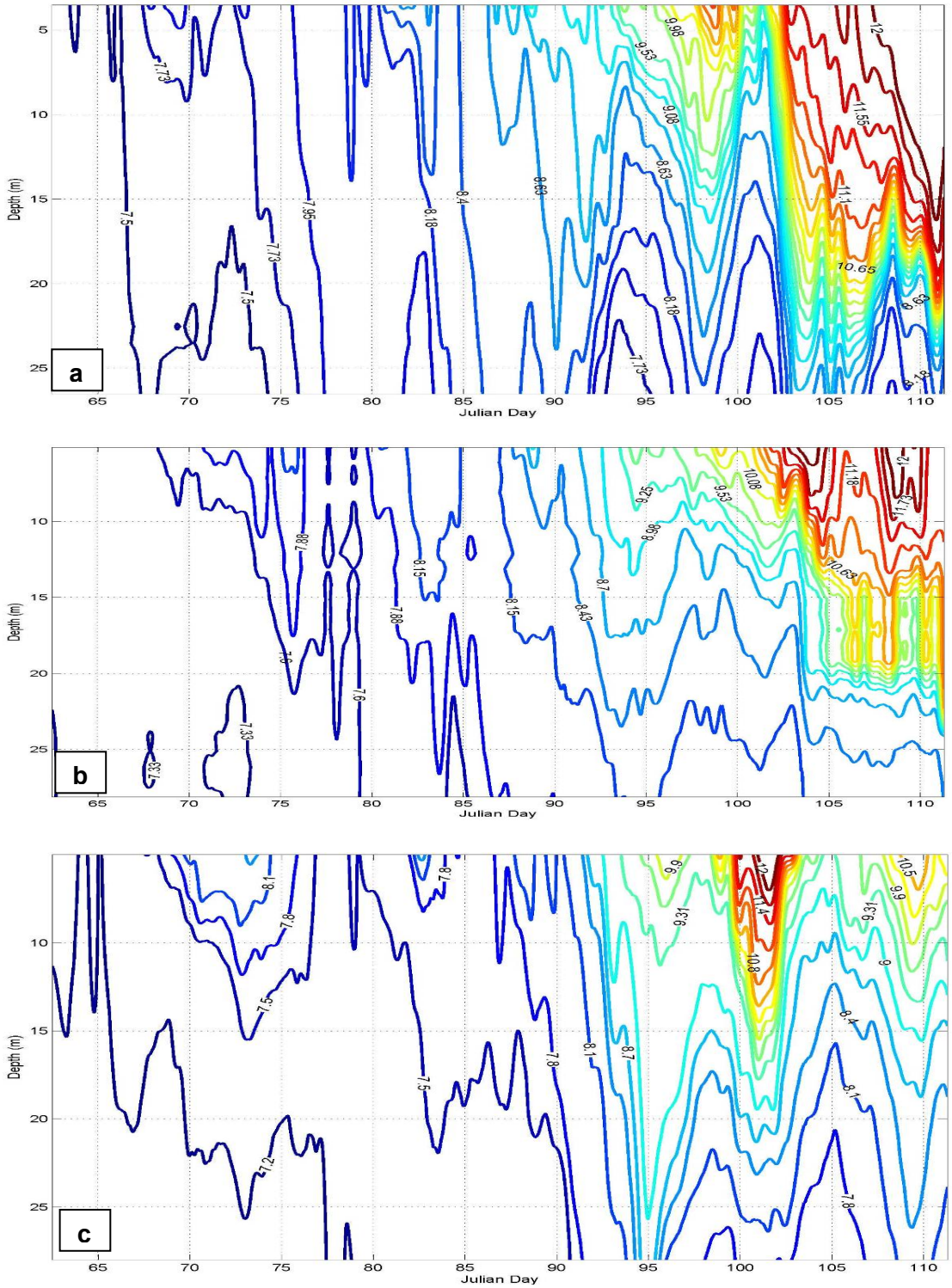

Figure 1. 27. For March 2004, temperature contour plots for location NOA (a), MWY (b) and SWA (c). Isotherms occur at ~0.22 °C intervals.

1.3.2 Longitudinal Temperature and Fluorescence Profiles

While the principal component analysis provided a general description of the vertical and horizontal distribution in temperature, more specific isotherm tilting was obtained from the SCAMP temperature profiles, and fluorescence profiles provided estimates of vertical mixing depths. The vertical mixing depth was defined as the point where coincident inflection points occurred in the fluorescence and temperature profiles.

1.3.2.1 2003 Observations

On March 27, 2003, temperatures at NOA were about one degree cooler than SWA and the isotherms were substantially tilted upward from north to south (Figure 1. 28). On this day, the warmest temperature at SWA (about 8.42 ^{o}C) was less than the coolest temperature at NOA (about 8.62 ^{o}C). The 8.42 ^{o}C isotherm surfaced near SWA and terminated at about 42 meters 5km south of NOA, and fluorescence was uniform to 42 meters at NOA and to 20 meters at SWA (Figure 1. 28 and Figure 1. 29). Fourteen days later on April 10 (JD 99.5), the isotherms were tilted upward from north to south with the 9.16 ^{o}C surfacing near SWA and depressed to 35 meters at NOA (Figure 1. 30). On this day at NOA, fluorescence was fairly uniform from 5 to 40 meters, and at SWA it was fairly uniform from 5 to 10 meters with some uniformity to 15 meters below a shoulder at 10 meters (Figure 1. 31). On May 1, the isotherms had a much shallower upward tilt from north to south with the 10.71 ^{o}C isotherm near 10 meters at SWA and near 15 meters at NOA (Figure 1. 32). The isotherm tilt would create the density difference observed in the average density time series (Figure 1. 17).

Based on the observed isotherm tilt between JD 88.5 and 99.5, the isotherms tilted upward from before JD 92.5 to about JD 111.5 when down welling occurred at SWA and upwelling occurred at SR520 (Figure 1. 17 and Figure 1. 21). The upward tilt is evident in the 8.63 ^{o}C isotherm, which was near 30 meters at SR520 and above 5 meters at SWA from JD 92.5 to 99 when it dipped to 15 meters near JD 104 and rose to 12 meters near JD 106, and finally dipped below 29 meters near JD 111 (Figure 1. 21). This isotherm tilt created a longitudinally varying mixed layer depth, which was 42 meters deep at NOA and about 20 meters deep at SWA on March 27 (Table 1. 8). The longitudinal variation was persistent through JD 108, but decreased significantly near JD 120 (Table 1. 8).

Based on the fluorescence and temperature profiles, the mixed layer depth, or depth to the density interface, ranged from 27 to 10 meters over the time of observations for year 2003 (Table 1. 8). Isotherms tilted upward from north to south prior to JD 92 and to JD 111; the tilt resulted in a longitudinally variable mixed layer depth.

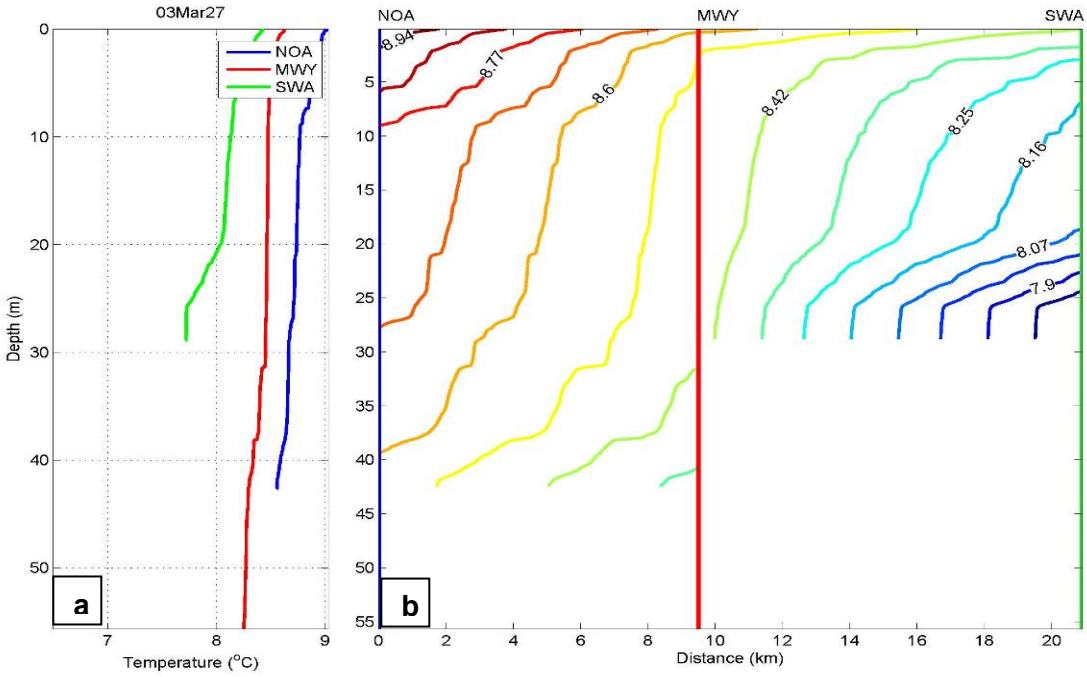

Figure 1. 28. Temperature profiles at the NOA (blue), MWY (red), and SWA (green) locations for March 27, 2003 (JD 85.5); (a) shows each profile and (b) shows isotherm contours based on the relative distance between locations; blue locates NOA, red MWY and green SWA. Temperatures increase from south to north (a) and isotherms have an upward tilt from north to south (b).

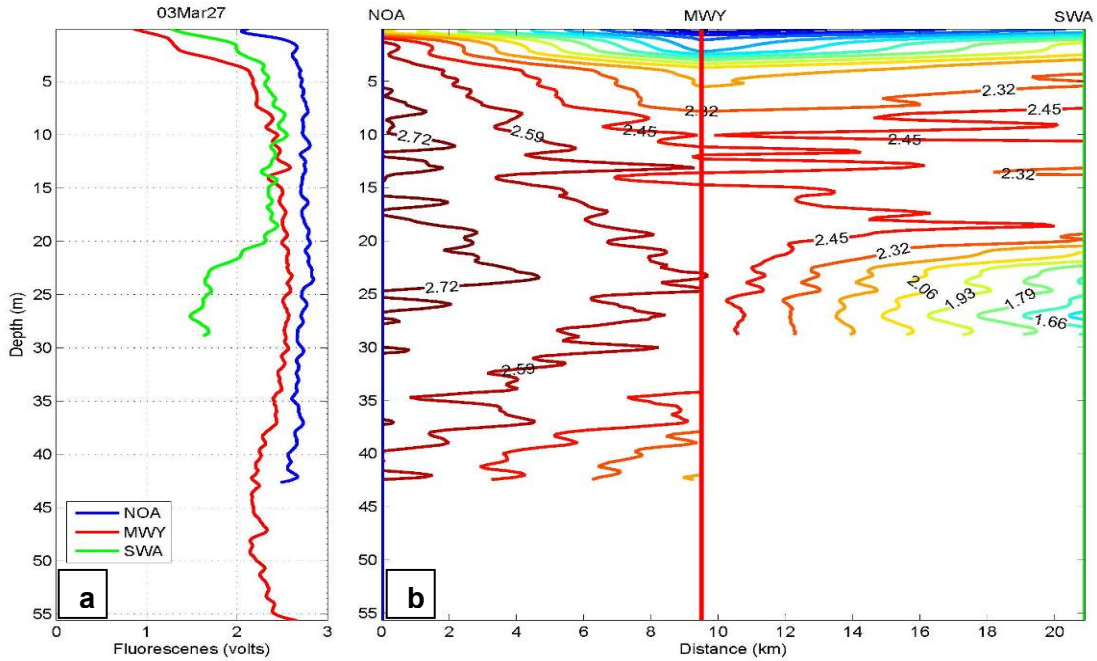

Figure 1. 29. Fluorescence profiles at the NWA (blue), MWY (red), SWA (green) locations for March 27, 2003 (JD 85.5); (a) shows each profile and (b) shows fluorescent contours based on the relative distance between locations; blue locates NOA, red MWY, and green SWA. Fluorescence increased slightly from south to north (a) and contours have an upward tilt from north to south (b).

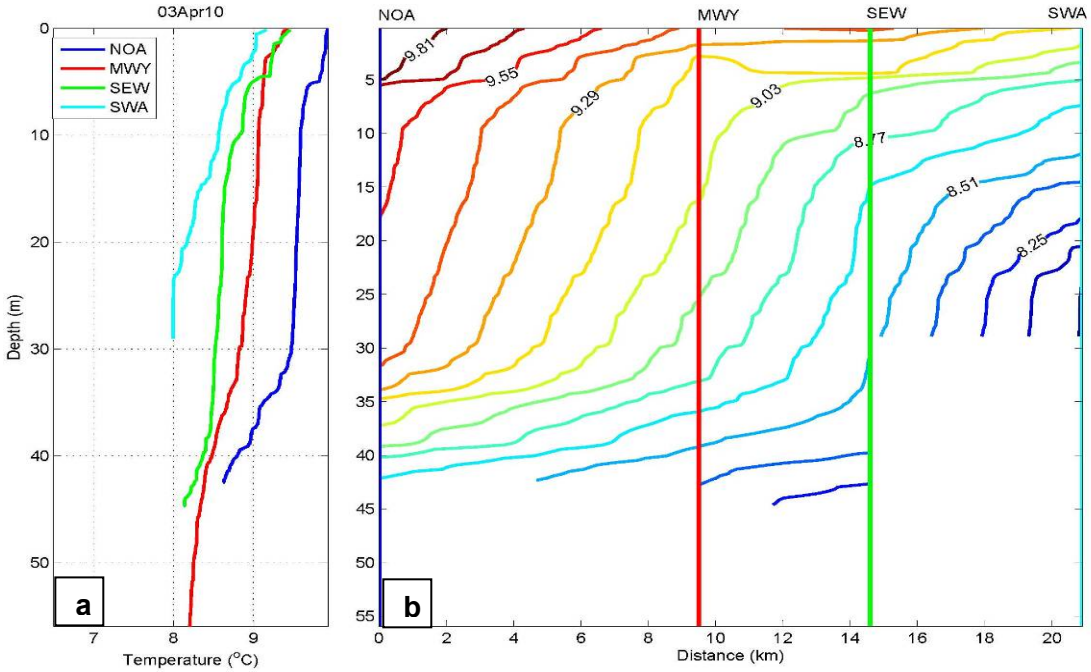

Figure 1. 30. Temperature profiles at the NOA (blue), MWY (red), SEW (green), SWA (cyan) locations for April 10, 2003 (JD 99.5); (a) shows each profile and (b) shows isotherm contours based on the relative distance between locations; blue locates NOA, red MWY, green SEW, and cyan SWA. Temperatures increase from south to north (a) and isotherms have an upward tilt from north to south (b).

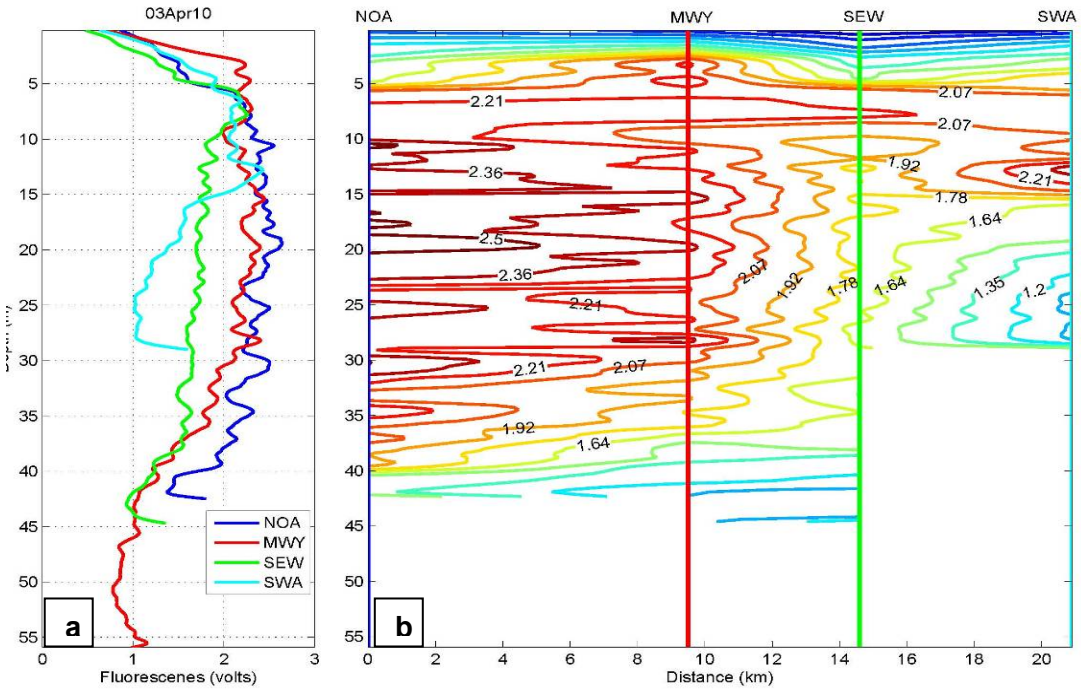

Figure 1. 31. Fluorescence profiles at the NWA (blue), MWY (red), SEW (green), SWA (cyan) locations for April 10, 2003 (JD 99.5); (a) shows each profile and (b) shows fluorescent contours based on the relative distance between locations; blue locates NOA, red MWY, green SEW, and cyan SWA. Fluorescence increased from south to north (a) and contours have an upward tilt from north to south (b).

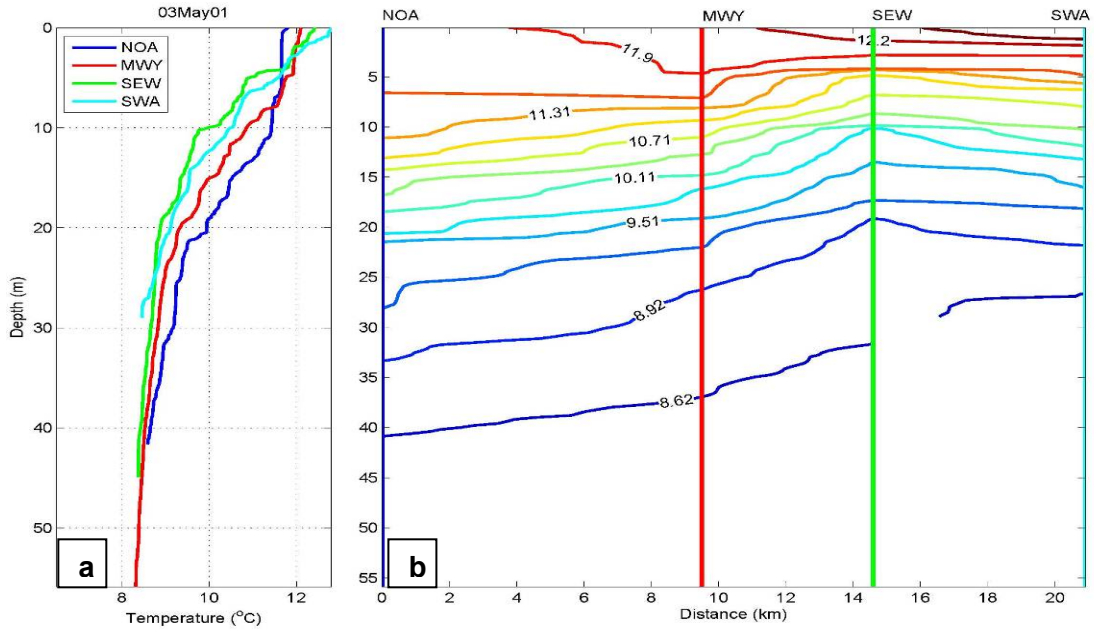

Figure 1. 32. Temperature profiles at the NOA (blue), MWY (red), SEW (green), SWA (cyan) locations for May 1, 2003 (JD 120.5); (a) shows each profile and (b) shows isotherm contours based on the relative distance between locations; blue locates NOA, red MWY, green SEW, and cyan SWA. Temperatures increase from south to north (a) and isotherms have an upward tilt from north to south (b).

Table 1. 8 Mixed layer depth based on Fluorescence and Temperature for 2003. The mean depth approximates the depth of the thermocline. Depths were based on coincident inflection points in the fluorescence and temperature profiles.

Date (JD)	Location			
	NOA	MWY	SWA	Mean Depth
March 27 (85.58)	42	38	20	29
April 10 (99.5)	35	30	15	27
May 1 (120.5)	12	10	10	10

1.3.2.2 <u>2004 Observations</u>

On March 2, 2004 a substantial isotherm tilt was present; at NWA the temperature profile was uniform from 5 to 32 meters and isotherms tilted upward to SWA (Figure 1. 33). At SWA a step in temperature occurred near 10 meters with a mid-point temperature about 7.2 ^{o}C, which dropped to about 42 meters just north of MWY (Figure 1. 33a). The step is also present at SEW but dissipates by MWY; however, the step probably starts near 28 meters at MWY based on the 7.27 ^{o}C isotherm, which represents the start of the step (Figure 1. 33b). Fluorescence at SWA decreased near 10 meters concurrent with the temperature step (Figure 1. 34). At MWY, NOA, and NWA fluorescence was the same and uniform with depth. Based on temperature and fluorescence, the mixed layer depth varied from 10 meters at SWA to 42 meters at NOA (Table 1. 9); at MWY, a small step in fluorescence occurred near 41 meters and could reflect the temperature step associated with the 7.2 ^{o}C isotherm (Figure 1. 34). A very similar isotherm tilt was observed on March 9 (JD 68.5), and between the two dates the average density at NOA was consistently less than that at SWA (Figure 1. 35 and Figure 1. 23).

On March 16 (JD 75.5), the isotherms were tilted upward from north to south with steeper tilts between NWA and NOA and MWY and SEW (Figure 1. 36). The density interface (thermocline) is about 34 meters at NWA, about 20 meters at MWY, and about 8 meters at SWA (Figure 1. 36). These thermocline depths are consistent with uniform fluorescence profiles. Fluorescence is uniform to about 34 meters at NWA, to about 20 meters at MWY, and to about 8 meters at SWA (Figure 1. 37). The mixed layer depth varied from 34 meters at NWA to 8 meters at SWA (Table 1. 9). Also, the warmer surface layer observed on March 2 and 9 was not present on days March 16 and 30, and the average density at NOA was less than the average density at SWA.

Isotherms tilted upward on March 30 (JD 89.5) and at MWY the thermocline was near 10 meters as distinguished by a temperature step at 10 meters (Figure 1. 38). At the temperature step the mid-point temperature is about 8.39 ^{o}C, which was near 32 meters at NOA, 10 meters at MWY, and surfaced about 4 km north of SWA (Figure 1. 38). However, the temperature-based mixed layer depth was difficult to corroborate with fluorescence profiles. Fluorescence at NOA breaks near 25 meters, either 10 or 22 meters at MWY, and near 20 meters at SWA (Figure 1. 39). The average density at NOA was less than that at SWA (Figure 1. 23). During this time interval the 7.5 ^{o}C isotherm was below 25 meters at NOA and above 20 meters at SWA (Figure 1. 27). Based on these findings and the average density series, the isotherms tilted upward from about JD 74 to 92 (Figure 1. 23).

Between about JD 92 and 100, the NOA and SWA average density series oscillated about each other (Figure 1. 23) and the SCAMP temperature profiles show the isotherms changed between an upward tilt from north to south to upward from south to north. On April 6 (JD 96.5), temperature profiles at all locations were nearly the same except for a portion of the SEW and SWA profiles, which may be explained by the isotherm displacements that indicate second mode vertical and first mode horizontal internal seiche. The 8.8 ^{o}C isotherm tilted slightly upward tilt from south to north while the 8.02 ^{o}C isotherm tilted slightly downward from south to north (Figure 1. 40). Not shown, the fluorescence profiles indicated a mixed layer depth of 20 meters at SWA and about 12 meters at NWA, which is coincident with the 8.8 ^{o}C isotherm (Figure 1. 40). On April 9 (JD 99.5), the temperature profiles were similar again and a slight amount of upwelling was observed between NWA and NOA and down welling between SEW and SWA (Figure 1. 41). This pattern is indicative of the initial response to a surface wind stress applied in the southward direction (Imberger, 1985). JD 99.5 is just before the average densities change and SWA becomes less than NOA (Figure 1. 23), which is indicative of an upward tilt from south to north. After about JD 102, the average density at NOA was less than at SWA (Figure 1. 23).

Isotherms tilted upward from north to south after JD 102. On April 13 (JD 103.5), isotherms tilted upward from north to south and the average density at NOA was less than that at SWA (Figure 1. 42 and Figure 1. 23). At SWA a large temperature step

occurred near two meters with a mid-point value of about 10.5 °C; the 10.5 °C isotherm was near two meters at SWA and near 16 meters at NWA (Figure 1. 42). On April 16 (JD 106.5), isotherms tilted upward from north to south and the average density at NOA was less than that at SWA (Figure 1. 43 and Figure 1. 23). At NWA a large temperature step occurred near 20 meters with a mid-point value near 11 °C; the 11.04 °C isotherm was near 20 meters at NWA, 8 meters at MWY, and surfaced about 5 km north of SEW (Figure 1. 43). Fluorescence was uniform to about 20 meters at NWA and at SWA peak fluorescence started to decay near 12 meters (Figure 1. 44). The mixed layer depth varied from 20 meters at NWA, 15 meters at MWY, and 12 meters at SWA (Table 1. 9).

Based on temperature and fluorescence profiles, the mixed layer depth or density interface depth ranged from 28 to 15 meters over the observed time interval for year 2004 (Table 1. 9). Isotherms tilted upward from north to south for extended time intervals between JD 61 and 70, 72 and 92, and after JD 101; the tilt resulted in a longitudinally variable mixed layer depth.

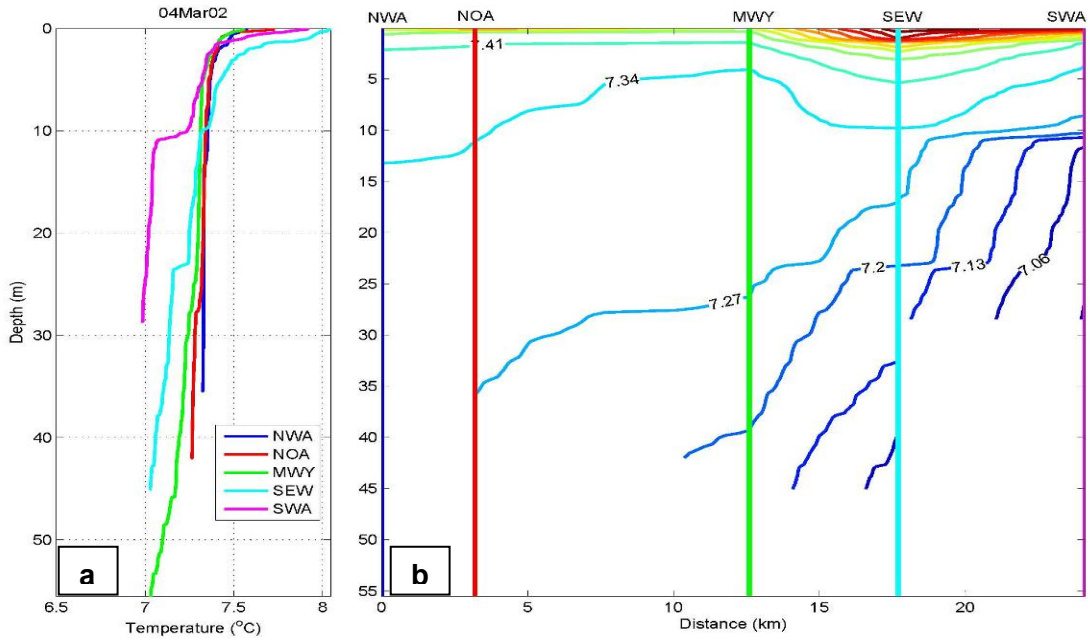

Figure 1. 33. Temperature profiles at the NWA (blue), NOA (red), MWY (green), SEW (cyan), and SWA (magenta) locations for March 2, 2004 (JD 61.5). Observed profiles (a) and isotherm contours based on the relative distance between locations (b), vertical lines identify station location. Temperature increased from south to north (a) and isotherms have an upward tilt from north to south (b).

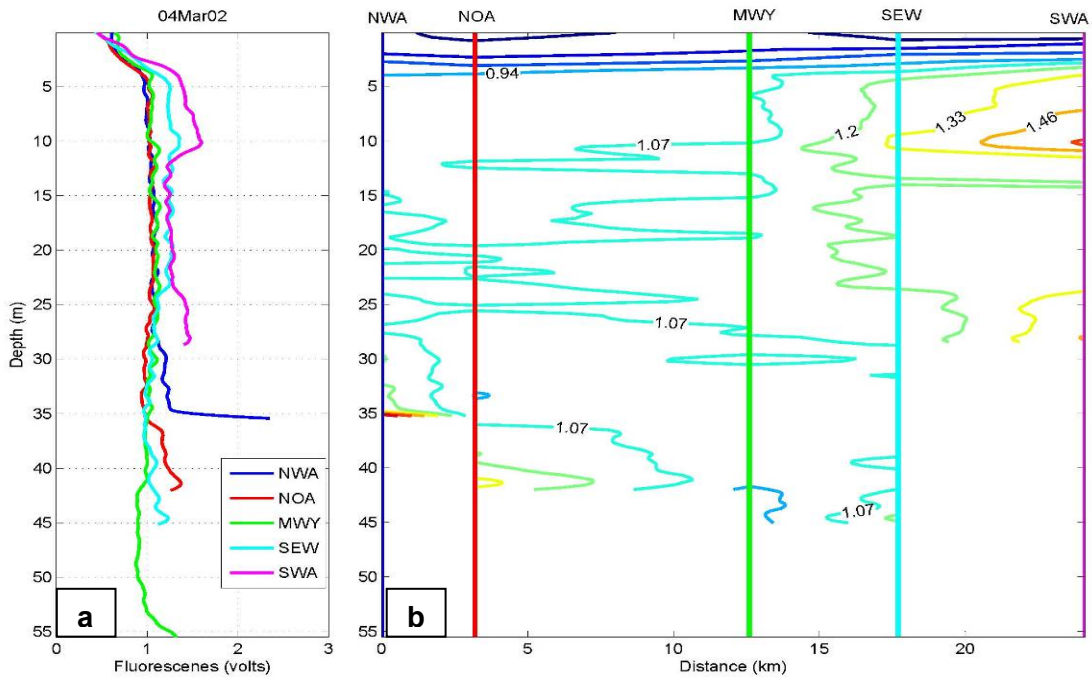

Figure 1. 34. Fluorescence profiles at the NWA (blue), NOA (red), MWY (green), SEW (cyan), and SWA (magenta) locations for March 2, 2004 (JD 61.5). Observed profiles (a) and fluorescence contours based on the relative distance between locations (b); vertical lines identify station location.

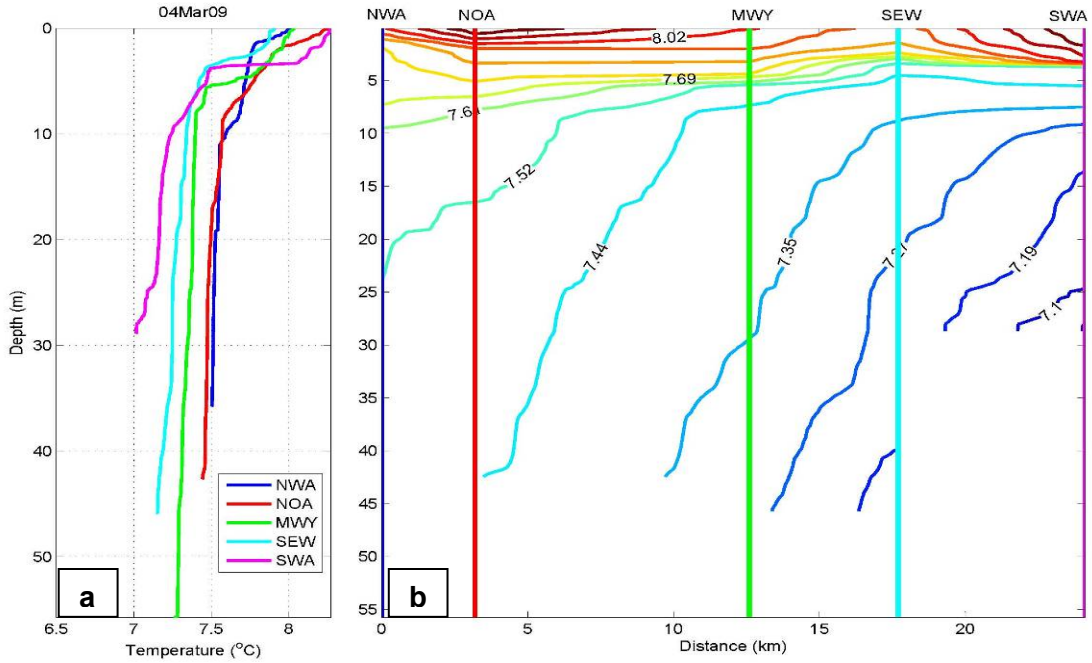

Figure 1. 35. Temperature profiles at the NWA (blue), NOA (red), MWY (green), SEW (cyan), and SWA (magenta) locations for March 9, 2004 (JD 68.5). Observed profiles (a) and isotherm contours based on the relative distance between locations (b); vertical lines identify station location. Temperature increased from south to north (a) and isotherms have an upward tilt from north to south (b).

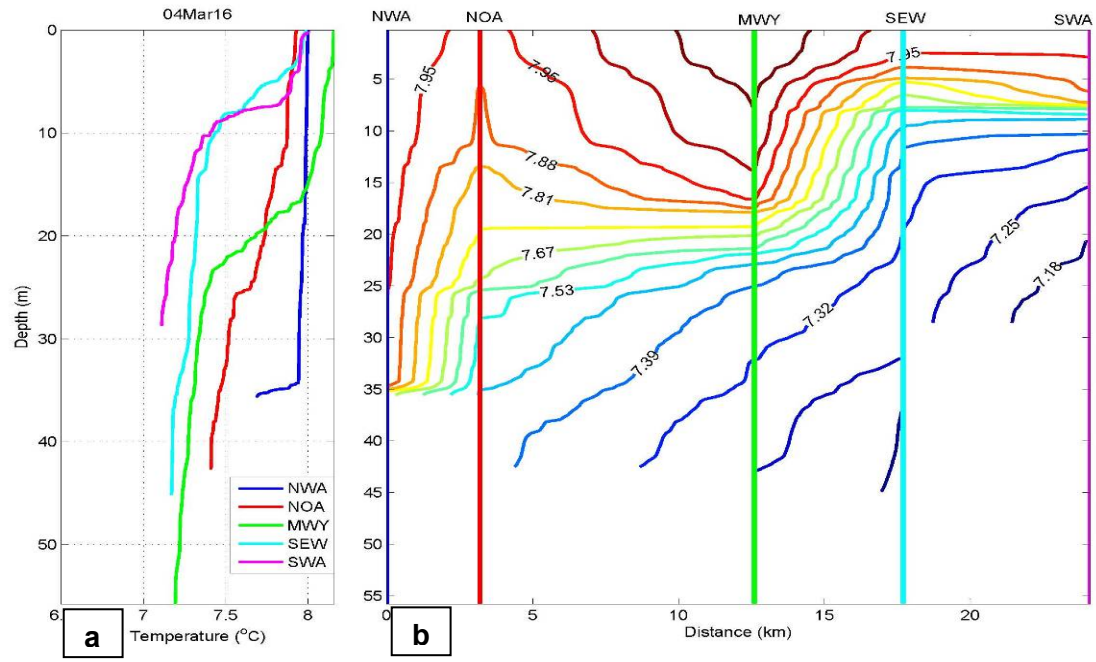

Figure 1. 36. Temperature profiles at the NWA (blue), NOA (red), MWY (green), SEW (cyan), and SWA (magenta) locations for March 16, 2004 (JD 75.5). Observed profiles (a) and isotherm contours based on the relative distance between locations (b); vertical lines identify station location. Temperature increased from south to north (a) and isotherms have an upward tilt from north to south (b).

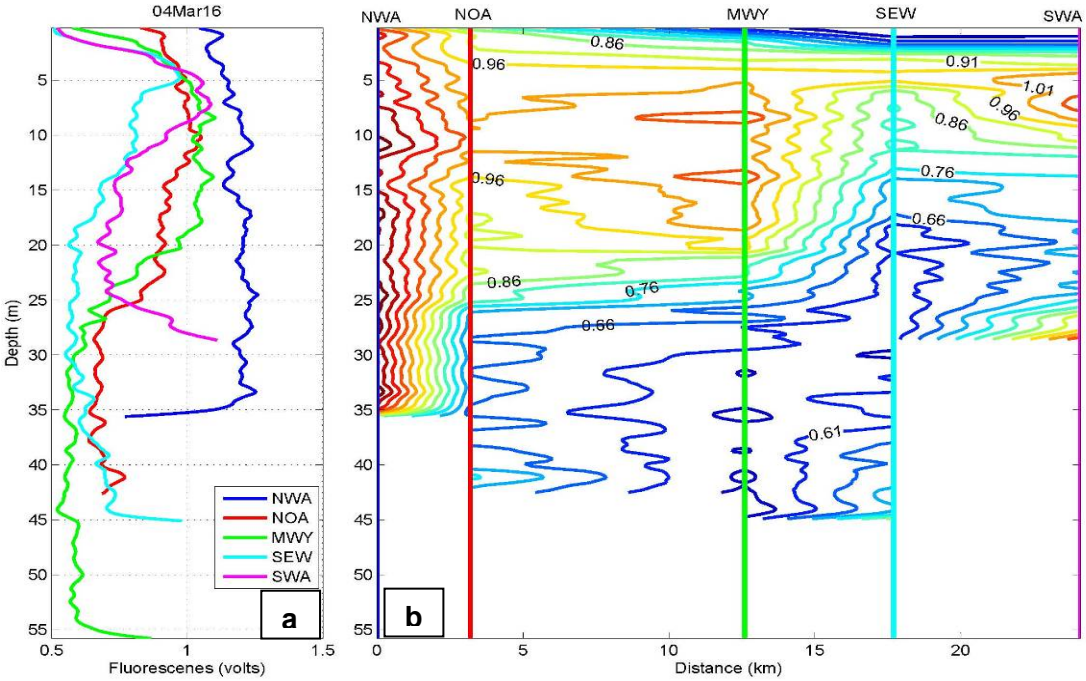

Figure 1. 37. Fluorescence profiles at the NWA (blue), NOA (red), MWY (green), SEW (cyan), and SWA (magenta) for March 16, 2004 (JD 75.5). Observed profiles (a) and fluorescence contours based on the relative distance between locations (b); vertical lines identify station location.

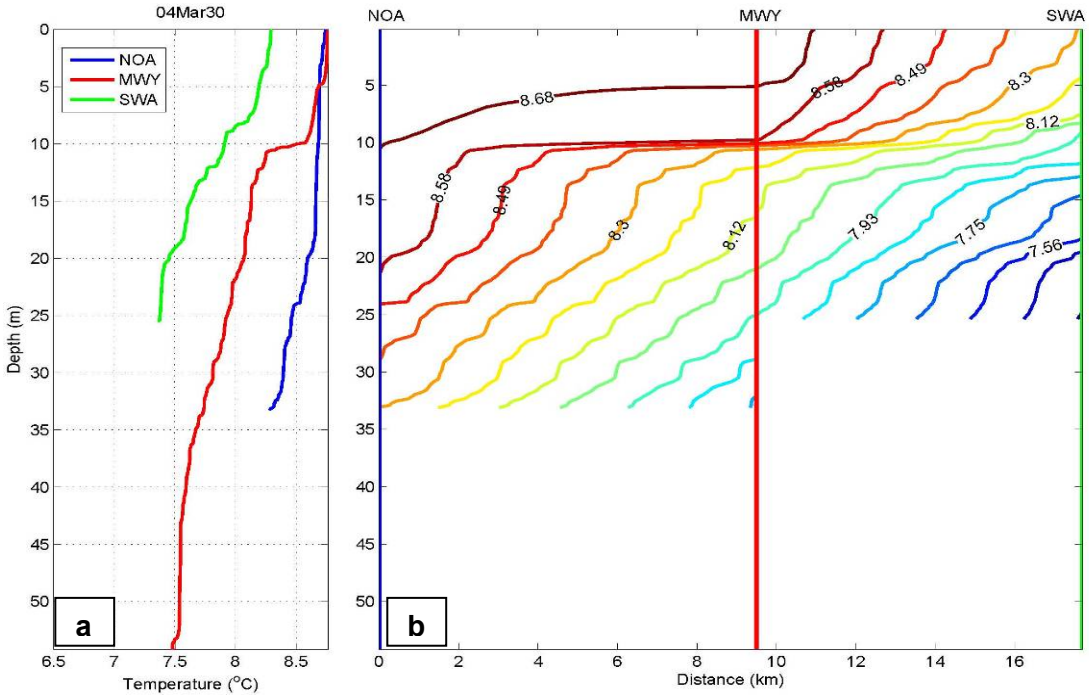

Figure 1. 38. Temperature profiles at the NWA (blue), NOA (red), MWY (green), SEW (cyan), and SWA (magenta) locations for March 30, 2004 (JD 89.5). Observed profiles (a) and isotherm contours based on the relative distance between locations (b); vertical lines identify station location. Temperature increased from south to north (a) and isotherms have an upward tilt from north to south (b).

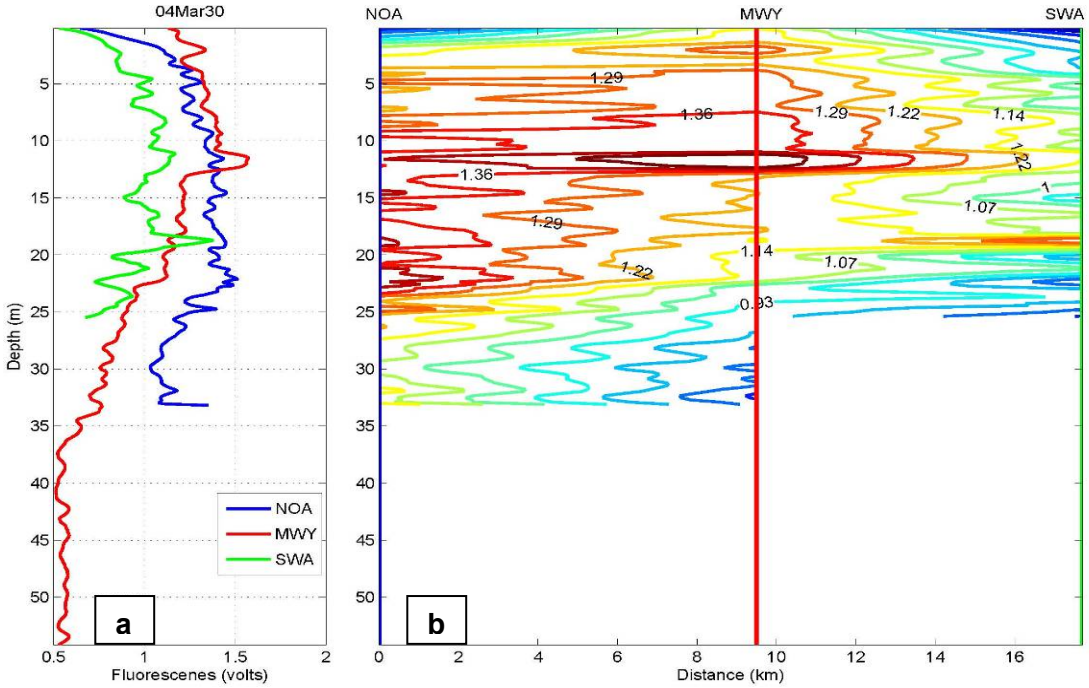

Figure 1. 39. Fluorescence profiles at the NWA (blue), NOA (red), MWY (green), SEW (cyan), and SWA (magenta) for March 30, 2004 (JD 89.5). Observed profiles (a) and fluorescence contours based on the relative distance between locations (b); vertical lines identify station location.

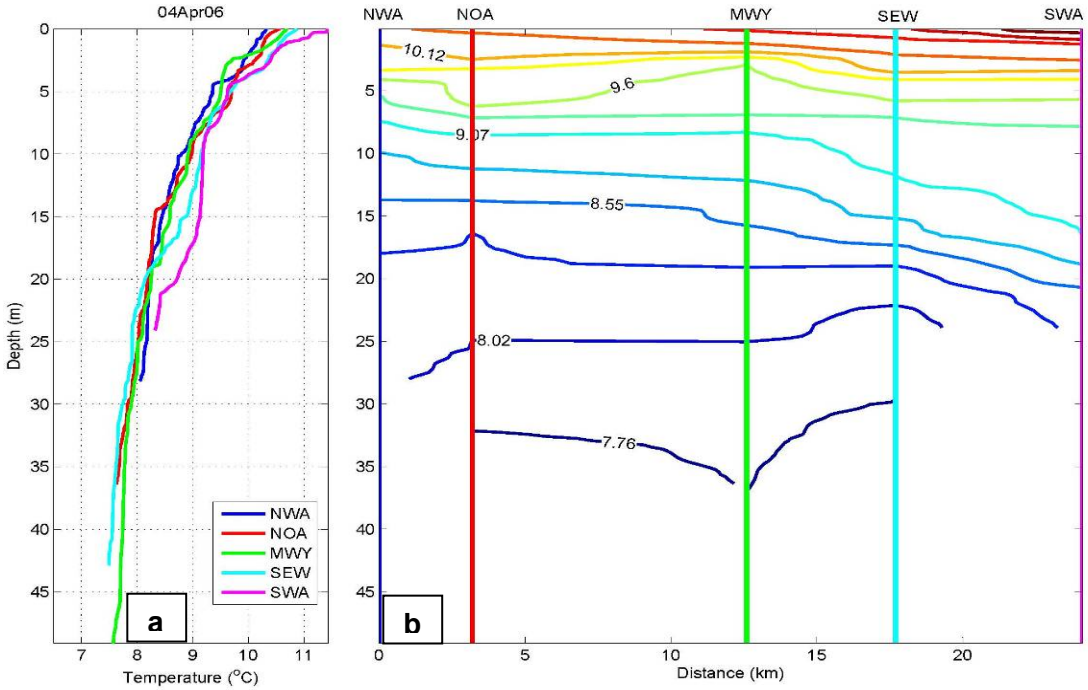

Figure 1. 40. Temperature profiles at the NWA (blue), NOA (red), MWY (green), SEW (cyan), and SWA (magenta) locations for April 6, 2004 (JD 96.5). Observed profiles (a) and isotherm contours based on the relative distance between locations (b); vertical lines identify station location. Temperature profiles indicate a slight south to north tilt.

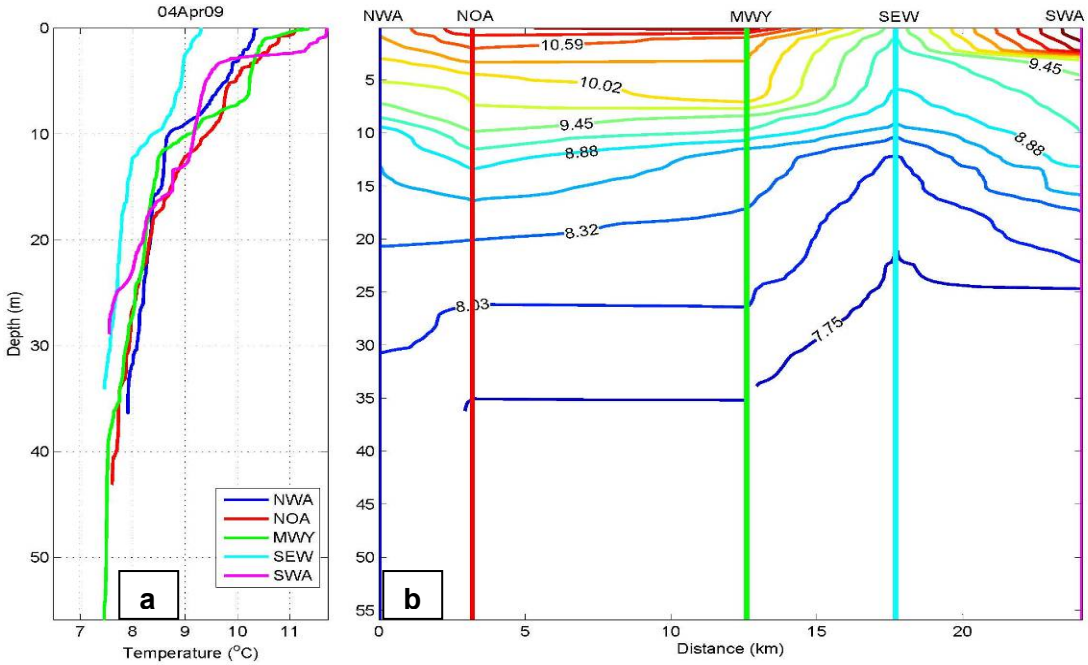

Figure 1. 41. Temperature profiles at the NWA (blue), NOA (red), MWY (green), SEW (cyan), and SWA (magenta) locations for April 9, 2004 (JD 99.5). Observed profiles (a) and isotherm contours based on the relative distance between locations (b); vertical lines identify station location. Temperature profiles indicate a neutral thermocline position.

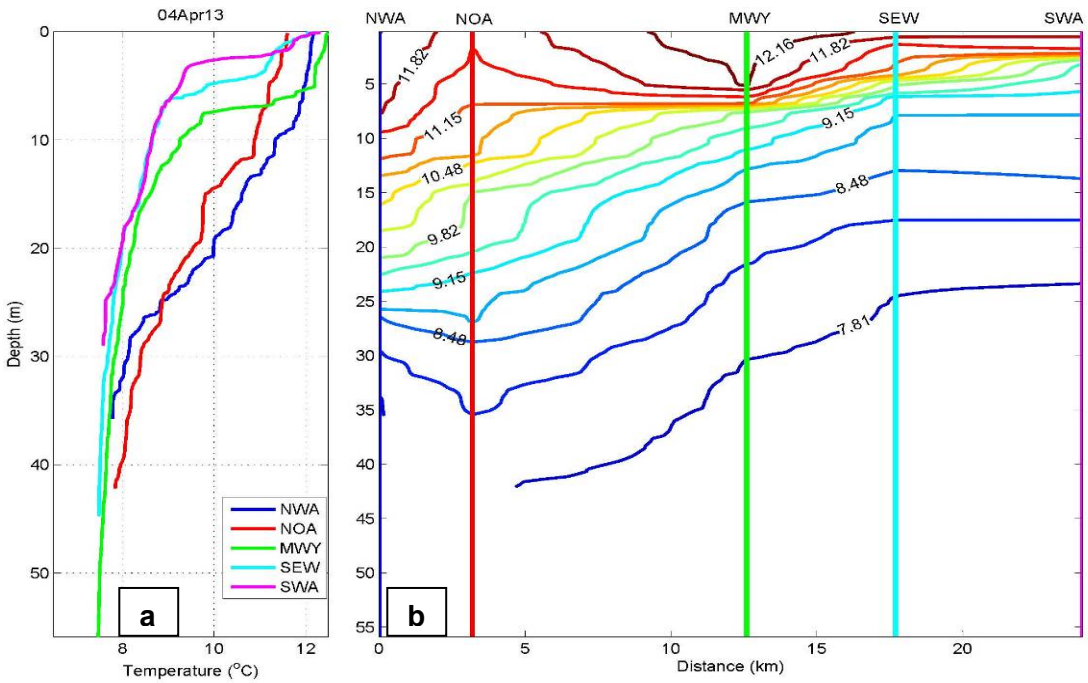

Figure 1. 42. Temperature profiles at the NWA (blue), NOA (red), MWY (green), SEW (cyan), and SWA (magenta) locations for April 13, 2004 (JD 103.5). Observed profiles (a) and isotherm contours based on the relative distance between locations (b); vertical lines identify station location. Temperature increased from south to north (a) and isotherms have an upward tilt from north to south (b).

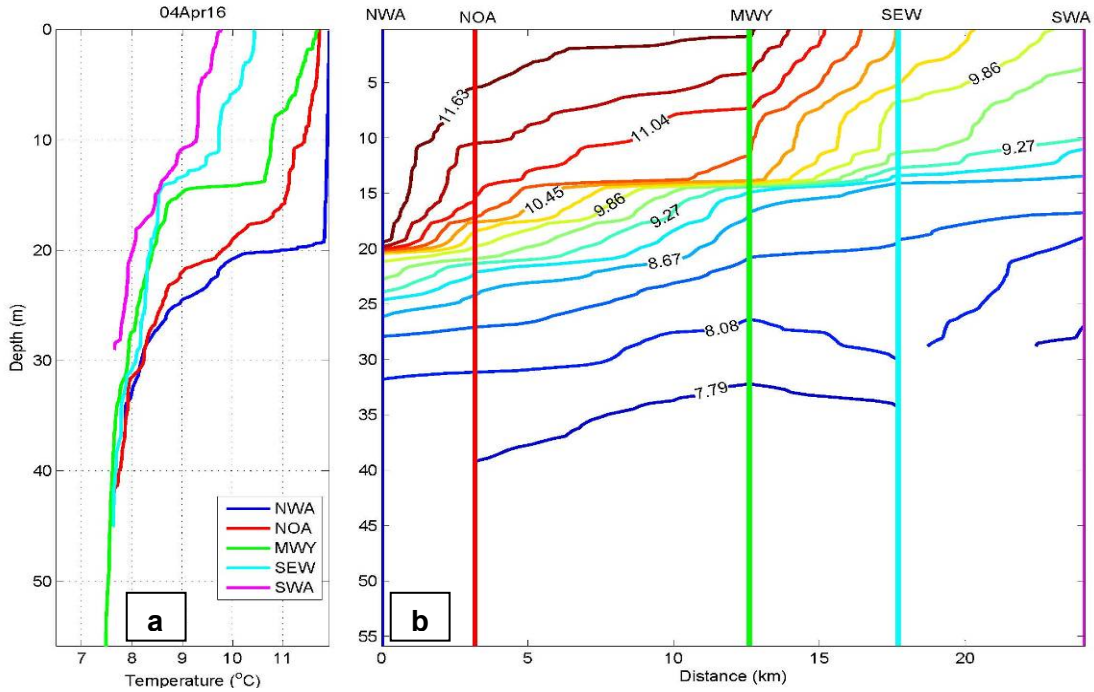

Figure 1. 43. Temperature profiles at the NWA (blue), NOA (red), MWY (green), SEW (cyan), and SWA (magenta) locations for April 16, 2004 (JD 106.5). Observed profiles (a) and isotherm contours based on the relative distance between locations (b); vertical lines identify station location.

Temperature increased from south to north (a) and isotherms have an upward tilt from north to south (b).

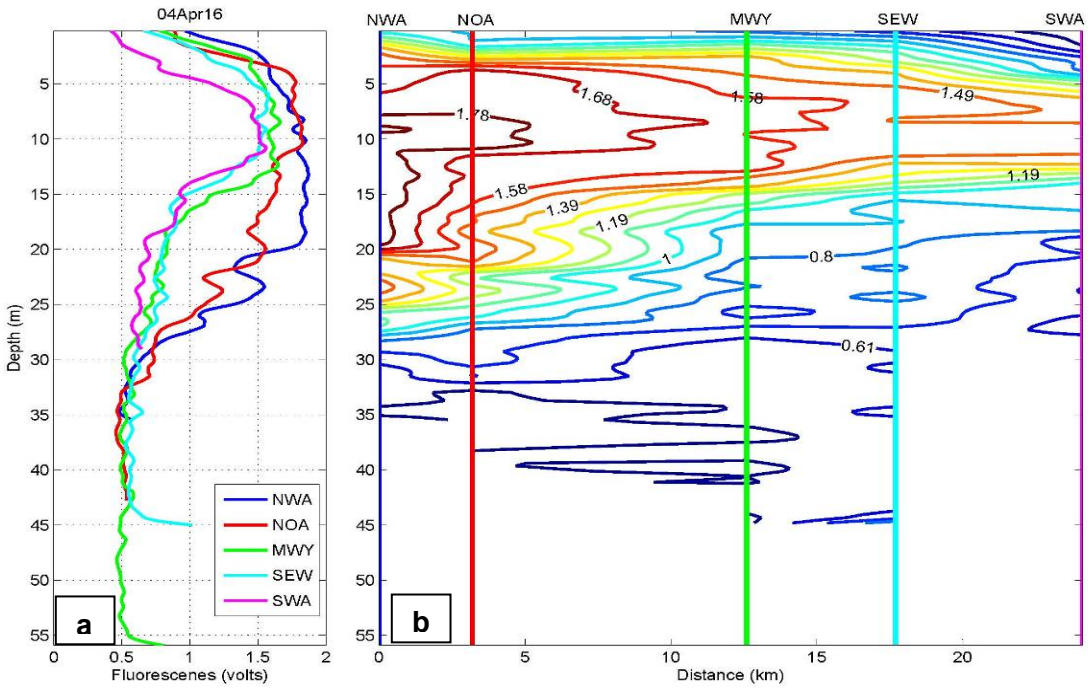

Figure 1. 44. Fluorescence profiles at the NWA (blue), NOA (red), MWY (green), SEW (cyan), and SWA (magenta) locations for April 16, 2004 (JD106.5). Observed profiles (a) and fluorescence contours based on the relative distance between locations (b); vertical lines identify station location.

Table 1. 9 Mixed layer depth based on Fluorescence and Temperature observations for 2004. The mean depth approximates the depth of the thermocline. Depths were based on coincident inflection points in the fluorescence and temperature profiles.

Date (JD)	NWA	NOA	MWY	SWA	Mean Depth
March 2 (61.5)	34*	42*	28	10	28
March 9 (68.5)	34*	42*	35	10	
March 16 (75.5)	34*	25	20	8	
March 30 (89.5)	NA	25	22	20	
April 16 (106.5)	20	20	15	12	15
* water depth at station					

1.3.3 Wedderburn and Lake Numbers and Relations between the Temperature and Velocity Expansion Coefficients

In this section, the Wedderburn and Lake Numbers are calculated and used to assess the relation between surface wind stress and isotherm tilting. In the previous sub-section, the principal component analysis showed that most of the information about the density perturbations (first mode expansion coefficients) could be explained by a first mode vertical and first mode horizontal type internal seiche response. Then the temperature and fluorescence analysis showed that the tilted

isotherms were manifested as a density difference between the north and south end of the lake. The tilted isotherms are the horizontal baroclinic pressure gradient represented in the Wedderburn Number. Thus, an analysis between the first mode expansion coefficients and the Wedderburn Number will provide information about the importance of surface wind stress in determining the isotherm tilt; the isotherm tilt creates the longitudinally varying mixed layer depth.

The Wedderburn Number was calculated by (1.7). Upper and lower layer density was estimated by methods described in §1.2.3.2. Upper layer depth (h_1) was estimated from the mixed layer depths presented in Table 1. 8 and Table 1. 9; the depth was allowed to vary linearly over time (Table 1. 10). The length L was equal to 31 km, which is the length of the lake near the 10-meter depth. Friction velocity was calculated by (1.3), with the 10-meter wind speed (U_{10}) obtained from the I-90 Bridge weather station (§1.2.2) and the drag coefficient determined by (1.17) (Johnson, Kim, and Nail, 2003).

$$C_D = 0.001\left(0.75 + 0.067U_{10}\right)$$
$$C_D \leq 0.003 \qquad (1.17)$$

The PCA and temperature profiles analyses showed that the isotherm response was indicative of a V1H1 internal seiche which has an expected period (T) defined by (1.6) for n=1. T/4 was used to determine the filter length for the low-pass saw-tooth filter applied to the friction velocity (§1.2.3.2); the average period T was used to determine the filter length. In 2003 the average period was 7.4 days and in 2004 it was 10.8 days.

Table 1. 10. Upper layer depths used to calculate the Wedderburn Number. The two values were used to determine the linear variation of h_1 over time for years 2003 and 2004.

	2003		2004	
	April 10 (JD 99.5)	May 1 (JD 120.5)	March 2 (JD 61.5)	April 16 (JD 106.5)
Upper Layer Depth (m)	27	10	28	15

The Lake Number was calculated by (1.10). Z_T was defined as upper layer depth (h_1) used in the Wedderburn Number (Table 1. 10). Z_G, Z_V, and m were estimated from the cell grid data file generated for the hydrodynamic model of Lake

Washington; the data contained cell area and depth information (Johnson, Kim, and Nail, 2003). The lake mass (m) also required density, which is described in §1.2.3.2.

When graphically comparing relations between wind, lake response, and the Wedderburn Number, Stevens et al. (1996) recommended using the friction velocity opposed to the wind speed; the wind speed does not capture the non-linear effects of momentum transfer with increasing wind speed. With the friction velocity, one cannot determine direction; therefore directional effects were represented as,

$$(u_{N*})^2 \propto |U| U_N \qquad (1.18)$$

Where |U| is the magnitude of the wind vector and U_N is the north wind vector component. Because Lake Washington is orientated north-south, $|U|U_N$ represented the dominant friction velocity or wind stress component along the north-south axis of the lake. In (1.18), a northward wind had a positive value and a southward wind had a negative value.

1.3.3.1 2003 Observations for Wedderburn and Lake Number, Temperature, and Wind Stress

Because the Wedderburn Number (W_N) is based on a scaling analysis, only order of magnitude differences can be considered significantly different; however, one can still assess relative changes in W_N and assess corresponding baroclinic changes in the lake. Therefore, the W_N time series was segmented into seven different periods when W_N changed in value and each period was reviewed to assess changes or effects in the lake; W_N=1 was the point of reference because it indicates a balance between surface wind stress and baroclinic pressure for the conceptual model.

The Wedderburn and Lake Numbers were of comparable value; neither number is substantially less than one nor greater than one, but both are considered small (<10). Large-scale tilting is expected for W_N and L_N less than one (Table 1. 5), which occurred for times before JD 98 and after JD 115 (Figure 1. 45). For times with W_N and L_N greater than one, small to medium amplitude seiching is expected (Table 1. 5). Because W_N and L_N are very similar, the Wedderburn Number will be used to assess relations between surface wind stress and baroclinic adjustments.

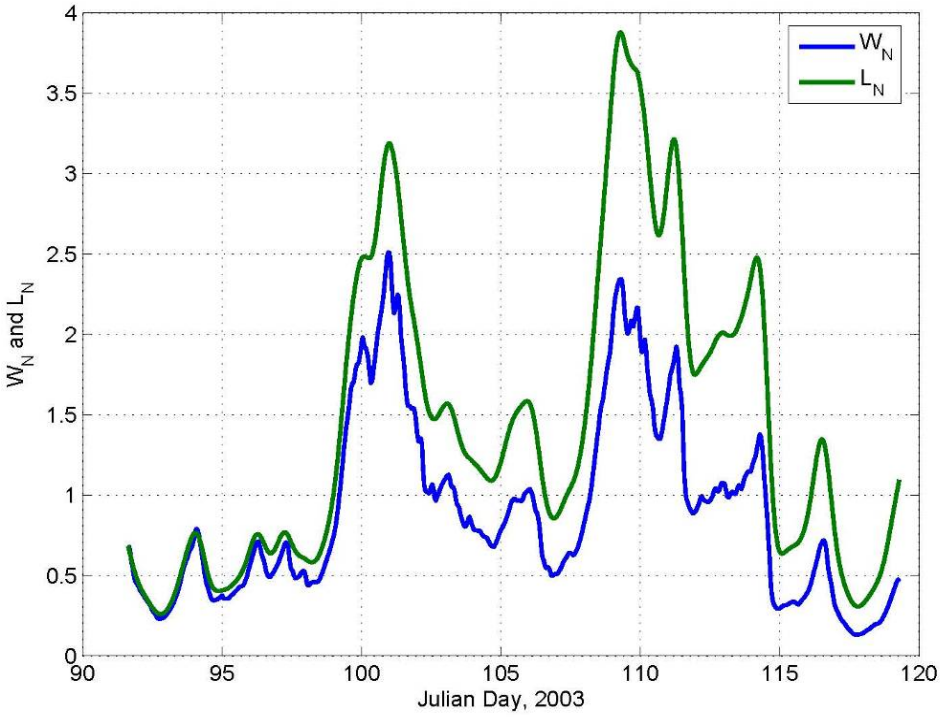

Figure 1. 45. Calculated Wedderburn and Lake Numbers for year 2003.

In 2003, six time intervals were identified where W_N was above or below one: Intervals P1 and P6 were less than one, P2 and P3 and P4 were greater than one, and P4 and P5 were near one (Figure 1. 46).

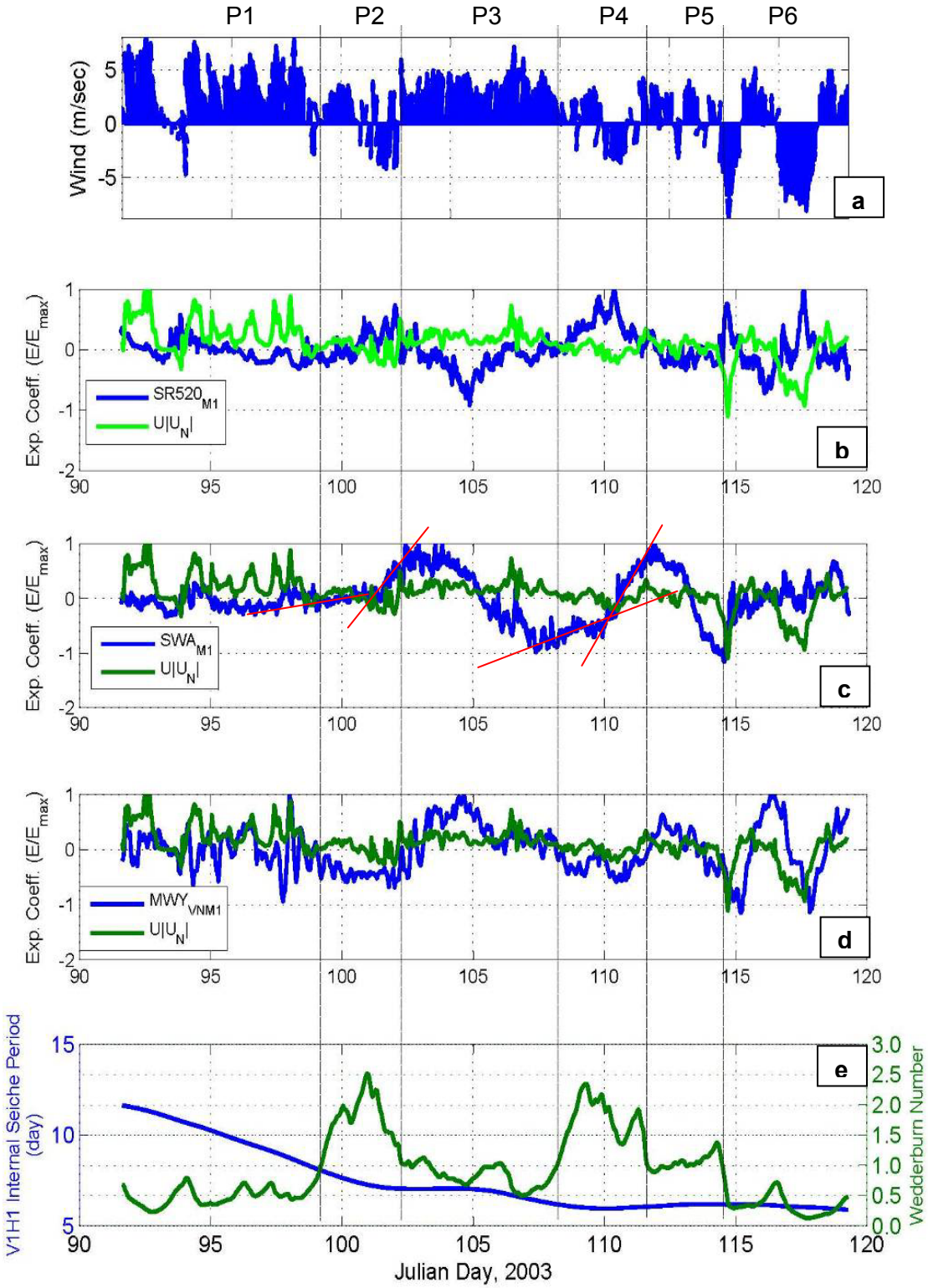

Figure 1. 46. Wind velocity vectors (a) and mode one expansion coefficients (blue lines) for SR520 (b), SWA (c), and MWY_{VN} (d); friction velocity is also shown (green line). Positive wind values mean it blows to the north. The Wedderburn Number (green line) and the period for a V1H1 internal seiche (blue line) are shown in (e). Red lines indicate instances when the wind stress shifted and complemented the density adjustment.

During P1, W_N was near 0.5 and the SR520 and SWA expansion coefficient remained fairly constant, but changes in W_N were reflected in the average density series. For W_N and L_N near 0.5, the surface wind stress would be expected to cause significant tilting of the thermal structure, which was evident prior to JD 85.5 (Figure 1. 28). The dynamic balance between wind and the baroclinic pressure was noted near JD 94 when W_N increased from about 0.25 to 0.75 (Figure 1. 46e). This adjustment was observed in the average density series; the SR520 and SWA densities converged because the reduced wind stress allowed a baroclinic adjustment, which relaxed the isotherm tilt.

Temperatures cooled at SWA while they warmed at SR520. During P1, wind events were periodic about one day apart with the longest about two days, but the V1H1 period was between 12 and 8 days with an average near 10 days (Figure 1. 46a and Figure 1. 46e). Linear theory suggests the tilted isotherms should relax to the neutral position in about 2.5 days. Since wind events occurred almost every day, the isotherm tilt had insufficient time to relax to a neutral position; the 8.63 ^{o}C isotherm was near 10 meters at SWA and near 30 meters at SR520 (Figure 1. 21).

During P2 W_N was greater than during P1 because wind stress decreased and the wind changed direction, which enhanced the baroclinic adjustment. As W_N increased, the SWA temperature expansion coefficients increased, which represents warming in the upper layer; concurrently, the average densities at SWA and SR520 converged (Figure 1. 17a and Figure 1. 46c). When the wind changed direction about mid-point in P2, the rate of change in temperature increased nearly five-fold over the rate of change prior to the change in direction (see red lines in Figure 1. 46c). While W_N is an order of magnitude estimator, it provides a good estimate of enhanced baroclinic adjustment. To compare acceleration effects from changing directions, before and after the direction change the rate of change in the expansion coefficients should correspond to changes in acceleration determined by (1.7). Prior to the change in direction $W_N \approx 1.75$, the wind opposes the baroclinic adjustment and (1.7) gives 1-1/1.75=0.43; at the change $W_N \approx 1.75$ but it enhanced the baroclinic adjustment and 1+1/1.75=1.57 and relative change in acceleration is 1.57/.43≈4, close to the five-fold change observed. Even though the wind stress enhanced the baroclinic adjustment, the duration was too short to allow the isotherms to relax to a

neutral position; the average density at SR520 was still less than at SWA (Figure 1. 17a).

During P3 the wind stress increased and W_N gradually decreased from one to less than one and the density difference between SR520 and SWA increased (Figure 1. 23). The larger wind stress increased the isotherm tilt, bringing cooler water to the surface at SWA and forcing warmer water down at SR520 (Figure 1. 21). The wind was fairly persistent and northward, and the temperature expansion coefficients decreased at SWA and increased at SR520 (Figure 1. 46).

During P4, wind stress decreased and winds reversed direction and again enhanced the baroclinic adjustment. W_N was greater than one and the average density at SR520 and SWA converged and temperature expansion coefficients increased at SWA (Figure 1. 46c). When the wind direction changed, the rate of temperature change at SWA increased dramatically (Figure 1. 46c) and the isotherms down welled rapidly (Figure 1. 21). At the end of P4, the isotherm adjusted to a nearly neutral position, the average density at SR520 and SWA were nearly equal, and isotherms were close to the same depth (Figure 1. 17 and Figure 1. 21).

During P5, the wind was northward and W_N was near one and the isotherms adjusted to an upward tilt from north to south. Temperature expansion coefficient decreased at SWA, isotherms upwelled at SWA, and average density at SR520 was less than at SWA (Figure 1. 46c, Figure 1. 21b, and Figure 1. 17).

During P6, the wind changed directions four times and W_N was near 0.5; however, the isotherms remained close to neutral position. At the start of P6, a strong southward wind quickly adjusted the isotherms near the neutral position (Figure 1. 17a and Figure 1. 21) While the SWA temperature expansions responded to the initial southward wind stress, after JD 115 the expansion coefficients responded very little to the large southward wind stress that occurred near JD 118; however, the mode two expansion coefficients had stronger adjustment (Figure 1. 46c and Figure 1. 19b). At MWY, the mode one velocity expansion coefficients were more significant than the mode two (Figure 1. 19c). Evidently, the MWY mode one velocity